INAM Plays a Critical Role in IFN-γ Production by NK Cells Interacting with Polyinosinic-Polycytidylic Acid–Stimulated Accessory Cells

Jun Kasamatsu,* Masahiro Azuma,*,[1] Hiroyuki Oshiumi,* Yuka Morioka,[†] Masaru Okabe,[‡] Takashi Ebihara,*,[2] Misako Matsumoto,* and Tsukasa Seya*

Polyinosinic-polycytidylic acid strongly promotes the antitumor activity of NK cells via TLR3/Toll/IL-1R domain–containing adaptor molecule 1 and melanoma differentiation-associated protein-5/mitochondrial antiviral signaling protein pathways. Polyinosinic-polycytidylic acid acts on accessory cells such as dendritic cells (DCs) and macrophages (Mφs) to secondarily activate NK cells. In a previous study in this context, we identified a novel NK-activating molecule, named IFN regulatory factor 3–dependent NK-activating molecule (INAM), a tetraspanin-like membrane glycoprotein (also called Fam26F). In the current study, we generated INAM-deficient mice and investigated the in vivo function of INAM. We found that cytotoxicity against NK cell–sensitive tumor cell lines was barely decreased in *Inam*$^{-/-}$ mice, whereas the number of IFN-γ–producing cells was markedly decreased in the early phase. Notably, deficiency of INAM in NK and accessory cells, such as CD8α$^+$ conventional DCs and Mφs, led to a robust decrease in IFN-γ production. In conformity with this phenotype, INAM effectively suppressed lung metastasis of B16F10 melanoma cells, which is controlled by NK1.1$^+$ cells and IFN-γ. These results suggest that INAM plays a critical role in NK-CD8α$^+$ conventional DC (and Mφ) interaction leading to IFN-γ production from NK cells in vivo. INAM could therefore be a novel target molecule for cancer immunotherapy against IFN-γ–suppressible metastasis. *The Journal of Immunology*, **2014, 193: 5199–5207.**

Microbial components play a major role in activating innate and adaptive immune responses by triggering pattern recognition receptors. Nucleic acid adjuvants, including polyinosinic-polycytidylic acid (polyI:C) and unmethylated CpG dinucleotides, strongly promote Th1 immune responses against cancer and infected cells and induce type I IFN and other inflammatory cytokines (1, 2). PolyI:C strongly enhances priming and expansion of Ag-specific T cells and NK cells with dramatic regression of syngeneic implant tumors in mice (3–6). NK cells belong to group 1 innate lymphocytes (ILC1s) and control progression of several types of tumors and microbial infections (7). Although polyI:C (an analog of viral dsRNA) is a ligand for multiple receptors, including dsRNA-dependent protein kinase, retinoic acid–inducible gene-I, melanoma differentiation–associated protein-5 (MDA5), and TLR3, both of the pathways initiated by TLR3/Toll/IL-1R domain–containing adaptor molecule 1 (TICAM-1) and MDA5/mitochondrial antiviral signaling protein confer antitumor activity on NK cells in vivo (8, 9).

PolyI:C also directly and indirectly activates human NK cells and other ILC1s (10, 11). PolyI:C participates in secondary activation of murine NK cells through stimulation of accessory cells such as dendritic cells (DCs) and other myeloid cells (12–14). In these interactions, previous studies have shown that type I IFN and cell contact via IL-15 receptors play a critical role in accessory cell activation followed by NK activation (15). In contrast, our previous studies showed that polyI:C induced bone marrow–derived DC (BMDC)–mediated NK cell activation through the TLR3/TICAM-1/IFN regulatory factor 3 (IRF3) pathway, which promoted antitumor immunity by adoptive transfer in a type I IFN- and IL-15–independent manner (8, 16). As the key molecule for this NK–DC interaction, we identified a novel IRF3-inducible tetraspanin-like membrane glycoprotein, named IRF3-dependent NK-activating molecule (INAM). INAM expression was induced not only in myeloid DCs but also in NK cells by polyI:C stimulation in vivo. Transfection of INAM in both BMDC and NK cells cooperated in inducing IFN-γ production and cytotoxicity against the NK-sensitive B16D8 cell line.

To investigate the role of INAM in vivo, we generated INAM-deficient mice by the standard gene-targeting method. INAM expression was induced not only in NK cells and conventional DC

*Department of Microbiology and Immunology, Graduate School of Medicine, Hokkaido University, Sapporo 060-8638, Japan; [†]Division of Disease Model Innovation, Institute for Genetic Medicine, Hokkaido University, Sapporo 060-8638, Japan; [‡]Research Institute for Microbial Disease, Osaka University, Osaka 565-0871, Japan

[1]Current address: Department of Pathology and Cellular Biology, Faculty of Medicine, University of Montreal, Montreal, QC, Canada.

[2]Current address: Department of Medicine, Howard Hughes Medical Institute, Washington University School of Medicine, St. Louis, MO.

Received for publication April 11, 2014. Accepted for publication September 9, 2014.

This work was supported in part by grants-in-aid from the Ministry of Education, Culture, Sports, Science and Technology and the Ministry of Health, Labor and Welfare of Japan, a Ministry of Education, Culture, Sports, Science and Technology of Japan Grant-in-Aid Project for Basic Research, "Carcinogenic Spiral," and the National Cancer Center Research and Development Fund (23-A-44). This work was also supported by the Takeda Science Foundation, the Yasuda Cancer Research Foundation, and the Iskra Foundation. J.K. is a Research Fellow of the Japan Society for the Promotion of Science.

Address correspondence and reprint requests to Prof. Tsukasa Seya, Department of Microbiology and Immunology, Graduate School of Medicine, Hokkaido University, Kita 15, Nishi 7, Kita-ku, Sapporo 060-8638, Japan. E-mail address: seya-tu@pop.med.hokudai.ac.jp

The online version of this article contains supplemental material.

Abbreviations used in this article: BMDC, bone marrow–derived DC; BST2, bone marrow stromal cell Ag 2; cDC, conventional DC; DC, dendritic cell; IFNAR1, IFN (α and β) receptor 1; ILC1, group 1 innate lymphocyte; INAM, IFN regulatory factor 3–dependent NK-activating molecule; IRF, IFN regulatory factor; Mφ, macrophage; MDA5, melanoma differentiation–associated protein-5; pDC, plasmacytoid DC; polyI:C, polyinosinic-polycytidylic acid; qPCR, quantitative real-time PCR; TICAM-1, Toll/IL-1R domain–containing adaptor molecule 1; WT, wild-type.

www.jimmunol.org/cgi/doi/10.4049/jimmunol.1400924

(cDC) subsets but also in other immune cells including macrophages (Mφs) and plasmacytoid DCs (pDCs) by polyI:C stimulation. Cytotoxicity against NK cell–sensitive tumor cell lines was barely decreased in *Inam*$^{-/-}$ mice, whereas the number of IFN-γ–producing cells markedly decreased in the early phase. We also showed that CD8α^{+} cDCs and Mφs facilitate secretion of IFN-γ from NK cells in response to polyI:C stimulation in vitro and in vivo. Notably, deficiency of INAM on NK and their accessory cells led to a robust decrease in IFN-γ production. Therefore, these results infer that INAM plays a critical role in the interaction of NK-CD8α^{+} cDCs (and Mφs) leading to IFN-γ production from NK cells. In agreement with this suggested phenotype, INAM effectively suppressed lung metastasis of B16F10 melanoma cells by controlling activation of NK1.1^{+} cells and IFN-γ. Taken together, these results provide the first demonstration, to our knowledge, that INAM plays a critical role in the interaction of NK–CD8α^{+} cDCs, which allows NK cells to produce IFN-γ. We propose in this study that INAM is a novel target molecule for immunotherapy against IFN-γ–suppressible tumors.

Materials and Methods

Mice

All mice were backcrossed with C57BL/6 mice more than seven times before use. A C57BL/6 background *Inam* (*Fam26f*)–targeted embryonic stem cell line, JM8A3.N1 of FAM26F tm2a (European Conditional Mouse Mutagenesis Program) Wtsi, was purchased from the European Conditional Mouse Mutagenesis Program. Chimeric mice were generated by aggregation of the mutated embryonic stem cells at the 8 cell stage. To remove exon 2 of *Inam*, the *Inam* heterozygous mutants were crossed with Cre-transgenic mice. The *Inam* heterozygous mutants obtained were intercrossed to obtain *Inam* homozygous mutants. *Ticam-1*$^{-/-}$ and *Mavs*$^{-/-}$ mice were generated in our laboratory (8, 16). *Irf-3*$^{-/-}$ and *Ifnar1*$^{-/-}$ mice were provided by Dr. T. Taniguchi (17). *Batf3*$^{-/-}$ C57BL/6 mice were purchased from The Jackson Laboratory (Bar Harbor, ME) (18). The *Batf3*$^{-/-}$ mice of C57BL/6 background [unlike 129 and BALB/c background (19)] lacked splenic CD8a^{+} DCs as described previously (18) and evoked insufficient T cell functional response against extrinsic Ag and adjuvant (Azuma et al., submitted for publication). C57BL/6 background were purchased from CLEA Japan (Shizuoka, Japan). Experiments were performed with sex-matched mice at 8–14 wk of age. All mice were bred and maintained under specific pathogen-free conditions in the animal facility of the Hokkaido University Graduate School of Medicine. Animal experimental protocols and guidelines were approved by the Animal Safety Center, Hokkaido University.

Semiquantitative RT-PCR and quantitative real-time PCR

Total RNA was extracted using TRIzol according to the manufacturer's instructions (Invitrogen). cDNA was generated by using the High Capacity cDNA Transcription Kit (ABI) with random primers according to the manufacturer's instructions. Quantitative real-time PCR (qPCR) was performed using the Step One Real-Time PCR system (ABI). The primer sequences for qPCR analysis were 5′-CAACTGCAATGCCACGCTA-3′ and 5′-TCCAACCGAACACCTGAGACT-3′ for *Inam*; 5′-TTAACTGAGGCTGGCATTCATG-3′ and 5′-ACCTACACTGACACAGCCCAAA-3′ for *Il15*; 5′-GACAAAGAAAGCCGCCTCAA-3′ and 5′-ATGGCAGCCATTGTTCCTG-3′ for *Il18*; 5′-ACCGTGTTTACGAGGAACCCTA-3′ and 5′-GGTGAGAGCTGGCTGTTGAG-3′ for *Irf7*; 5′-GCCGAGACACAGGCAAAC-3′ and 5′-CCAGGGCTTGAGACACCTTC-3′ for bone marrow stromal cell Ag 2 (*Bst2*); and 5′-GCCTGGAGAAACCTGCCA-3′ and 5′-CCCTCAGATGCCTGCTTCA-3′ for *Gapdh*. The primer sequences for semi-qPCR analysis were 5′-CAACTGCAATGCCACGCTA-3′ and 5′-TCCAACCGAACACCTGAGACT-3′ for *Gapdh*.

Mφ depletion and stimulation using TLR agonists in vivo

To generate Mφ-depleted mice, mice were injected i.p. with 150 μl Clophosome-Clodronate Liposomes (FormuMax). For qPCR analysis of *Inam* induction using some TLR antagonists in Fig. 1E, mice were injected i.p. with 50 μg polyI:C (GE Bioscience), 50 μg Pam3CSK4 (Boehringer Ingelheim), 10 μg LPS (Sigma-Aldrich), 50 μg R837 (InvivoGen), and 50 μg CpG ODN1826 (InvivoGen). In other experiments, polyI:C was injected i.p. at a dose of 200 μg/mouse.

Cells

For isolation of DC subsets, Mφs and NK cells, spleens were treated with 400 Mandle U/ml collagenase D (Roche) at 37°C for 25 min in HBSS (Sigma-Aldrich). EDTA was added, and the cell suspension was incubated for an additional 5 min at 37°C. NK cells were purified from spleens by positive selection of DX5-positive cells with DX5 MACS beads (Miltenyi Biotec). CD8α^{+} cDCs were purified using a CD8α^{+} DC isolation kit and CD11c MACS beads (Miltenyi Biotec). CD8α^{-} cDCs were purified with CD11c MACS beads (Miltenyi Biotec) from the negative fraction after CD8α^{+} cDC separation. F4/80^{+} Mφs were isolated using MACS-positive selection beads (Miltenyi Biotec) as described previously (13). pDC Ag-1^{+} pDCs were isolated with pDC Ag-1 MACS beads (Miltenyi Biotec). All immune cells were purified from spleens by repeated positive selection to achieve high purity (90%). Leukocytes from the lung were prepared as previously reported (18). Mouse immune cells were cultured in RPMI 1640/10% FCS/55 μM 2-ME/10 mM HEPES. B16D8, B16F10, YAC-1, and RMA-S were cultured in RPMI 1640/10% FCS.

Cell culture

To investigate potential interactions with NK–accessory cells, MACS-sorted accessory cells were cocultured with freshly isolated NK cells (accessory cells /NK = 1:2) with or without 20 μg/ml polyI:C for 24 h. In some coculture experiments using the transwell system, NK cells were added to 0.4-μm pore transwells (Corning) in the presence of polyI:C. Activation of NK cells was assessed by measuring the concentration of IFN-γ (ELISA; GE Healthcare) in the medium. For the IFN (α and β) receptor 1 (IFNAR1) blocking experiment, anti-IFNAR Ab at a final concentration of 10 μg/ml was added to the cultures before addition of polyI:C. For measurement of IL-12p40 and type I IFNs, we used ELISA kits purchased from BioLegend and PBL Biomedical Laboratories, respectively.

FACS analysis

For intracellular cytokine staining of NK cells, we isolated spleen or lung from polyI:C- or PBS-injected mice at each time point and harvested their leukocytes as described previously (18, 19). The leukocytes were incubated in medium with 10 μg/ml brefeldin A for 4 h. Cells were fixed and stained with a combination of anti-NK1.1 (PK136) and anti-CD3ε (145-2C11) Abs (BioLegend), followed by permeabilization and staining with anti-IFN-γ (XMG1.2) Ab (BioLegend), anti–granzyme B (NGZB) Ab (eBioscience), anti–TNF-α (MP6-XT22) Ab (BioLegend), anti–GM-CSF (MP1-22E9) Ab (BioLegend), or anti–IL-2 (JES6-5H4) Ab (BioLegend) using a BD Cytofix/Cytoperm Kit (BD Biosciences). For staining of the C terminus of INAM of each immune cell type, after treatment of anti-CD16/32 (no. 93), cell-surface molecules of splenocytes were stained with anti-CD3ε (145-2C11), anti-CD8α (53-6.7), anti-CD11c (N418), anti-NK1.1, anti-F4/80 (BM8), anti-Gr1 (RB6-8C5), anti-CD11b (M1/70), or anti-CD19 (MB19-1) Abs (BioLegend) or with anti-B220 (RA3-6B2) or anti-CD4 (L3T4) Abs (eBioscience). After staining of the cell surface, cells were fixed and permeabilized using a BD Cytofix/Cytoperm Kit (BD Biosciences) and then stained with an anti-INAM polyclonal Ab as described previously (16). To detect activating markers, NK receptors, and developmental markers, splenocytes were stained with anti-CD27 (LG.3A10), anti-CD25 (PC61), anti-NKp46 (29A1.4), anti-NKG2D (C7), anti-DNAM-1 (10E5), and anti-TRAIL (N2B2) Abs from BioLegend or anti-Fas (Jo2) from BD Biosciences. For detection of dead cells, samples were stained with ViaProbe from BD Biosciences. Samples were processed on an FACSCalibur flow cytometer and analyzed with FlowJo software (Tree Star).

Tumor inoculation and polyI:C treatment

PolyI:C therapy against mice with B16D8 tumor burden was described previously (8). B16F10 melanoma cells (2×10^5) were injected into wild-type (WT) or *Inam*$^{-/-}$ mice via the tail vein on day 0. PolyI:C was injected i.p. on days 1, 4, 7, and 10 at a dose of 200 μg/mouse. The control group was treated with PBS. All mice were killed 12 d after tumor inoculation. The lungs were excised and fixed in Mildform (Wako) for counting of surface colonies under a dissection microscope.

Statistical analysis

Statistical analyses were made with the Student *t* test for paired data. Statistical analyses were made with ANOVA in multiple comparisons. The *p* value of significant differences is reported.

Results

Generation of INAM-deficient mice

We designed a targeting vector to disrupt exon 2, which encodes the C-terminal transmembrane and cytoplasmic regions of INAM

(Fig. 1A). The heterozygosity and homozygosity of siblings were verified by Southern blot analysis (Fig. 1B). Mutant mice were born at the expected Mendelian ratio from *Inam*$^{-/-}$ and *Inam*$^{+/-}$ parents and showed normal healthy development under specific pathogen-free conditions (Fig. 1C). We also examined the composition of immune cells in the spleen and found no clear difference between WT and *Inam*$^{-/-}$ mice (Table I). Murine NK cells are divided into four subsets in their maturation stage based on the surface density of CD27 and CD11b: CD11b^{low}/CD27^{low}, CD11b^{low}/CD27^{high}, CD11b^{high}/CD27^{high}, and CD11b^{high}/CD27^{low} (20). We examined the composition of splenic NK cells in each maturation stage and found no clear difference between WT and *Inam*$^{-/-}$ mice (Supplemental Fig. 1A). A previous study showed that *Inam* mRNA is highly expressed in spleen and thymus under steady-state conditions

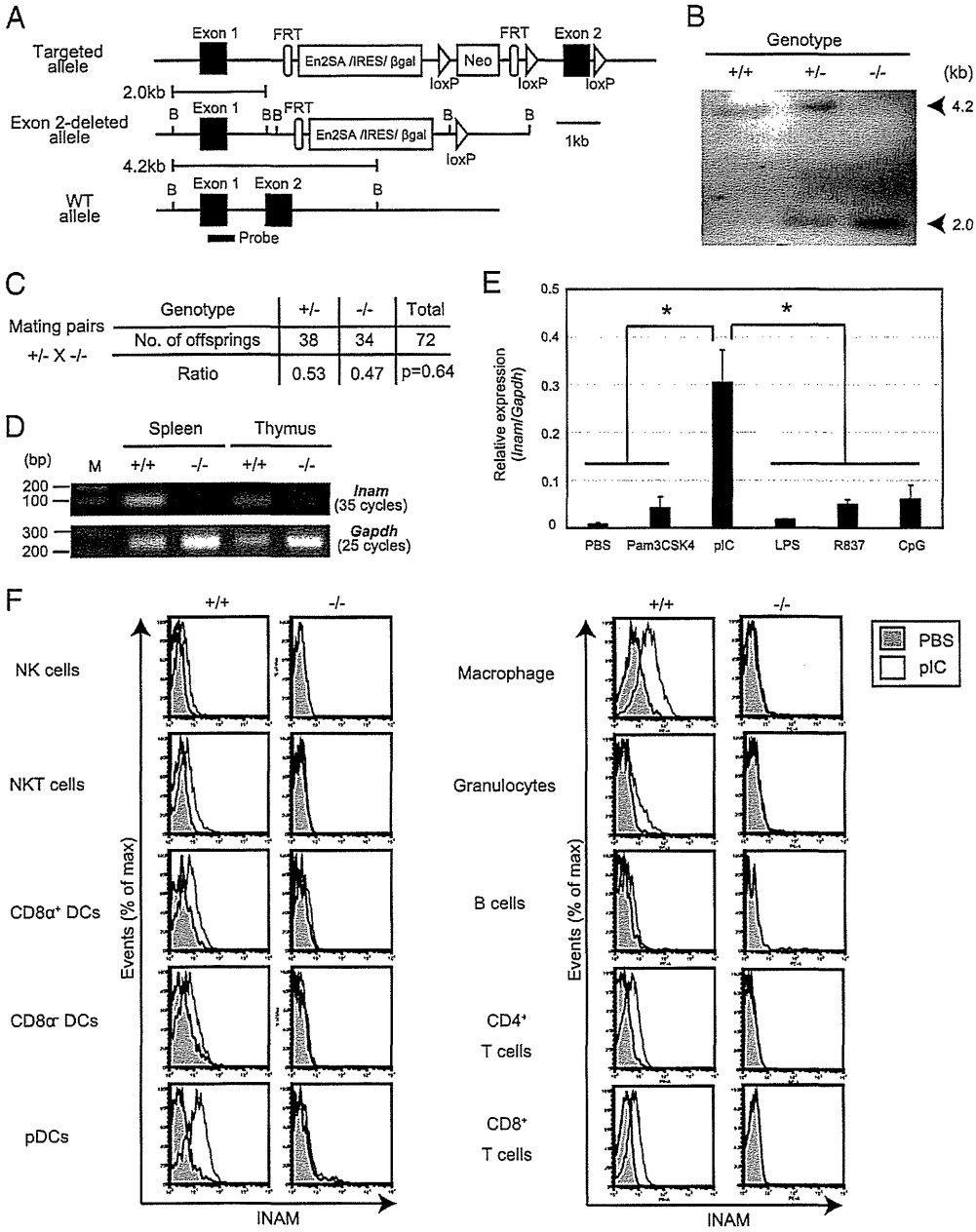

FIGURE 1. Generation of INAM-deficient mice. (**A**) Structure of the mouse *Inam*-targeted, *Inam*-disrupted, and WT allele. Closed boxes indicate the coding exon of Inam. A probe (602 bp) for Southern blot analysis was designed in exon 1. (**B**) Southern blot analysis of BamHI-digested genomic DNA isolated from WT (+/+), heterozygous mutant (+/−), and homozygous mutant (−/−) mice. (**C**) Genotype analyses of offspring from heterozygote intercrosses. The χ^2 goodness-of-fit test indicated that deviation from the Mendelian ratio was not statistically significant ($p > 0.1$). (**D**) RT-PCR analysis of spleen and thymus. Total RNA sets from spleen and thymus in WT (+/+) and *Inam*$^{-/-}$ (−/−) mice were extracted and subjected to RT-PCR to determine *Inam* expression. (**E**) *Inam* mRNA expression in response to TLR agonists. Total RNA were isolated from the spleens of mice in each group ($n = 3$) at 3 h after TLR agonist stimulation and subjected to quantitative PCR to determine to determine *Inam* expression. *$p < 0.05$ (**F**) INAM expression of immune cells. WT (+/+) and *Inam*$^{-/-}$ (−/−) mice were i.p. injected with 200 μg polyI:C (pIC) or PBS ($n = 2$). After 12 h, INAM expression of each immune cell type was analyzed by flow cytometry. Open histograms and shaded histograms indicate immune cells derived from the mice. Immune cells were classified as NK cells (CD3ε$^-$/NK1.1$^+$), NKT cells (CD3ε$^-$/NK1.1^{int}), B cells (CD19c$^+$/B220$^+$), CD8$^+$ T cells (CD3ε$^+$/CD8α$^+$), CD4$^+$ T cells (CD3ε$^+$/CD4α$^+$), classic CD8α$^-$ cDCs (CD11c^{high}/CD8α$^-$), classic CD8α$^+$ cDCs (CD11c^{high}/CD8α$^+$), pDCs (CD11c^{int}/B220$^+$), Mφs (CD11c$^{low\text{-}dim}$/CD11b$^{low\text{-}dim}$/F4/80$^+$), and granulocytes (CD11b^{high}/Gr-1$^+$). The data shown are representative of at least two independent experiments.

Table I. Development of hematopoietic cells in INAM-deficient mice

Cells	WT	*Inam*$^{-/-}$	Student *t* Test
CD4$^+$ T cells	16.9 ± 0.3	16.2 ± 2.2	$p = 0.69$
CD8$^+$ T cells	8.6 ± 0.5	8.0 ± 1.0	$p = 0.27$
B cells	55.6 ± 1.9	56.4 ± 3.5	$p = 0.65$
NK cells	1.2 ± 0.4	2.3 ± 0.7	$p = 0.22$
NKT cells	0.9 ± 0.1	0.76 ± 0.2	$p = 0.27$
pDCs	1.0 ± 0.1	1.0 ± 0.1	$p = 0.91$
CD8α$^+$ DCs	0.2 ± 0.01	0.3 ± 0.02	$p = 0.03$
CD8α$^-$ DCs	0.49 ± 0.03	0.8 ± 0.2	$p = 0.09$
Granulocytes	0.3 ± 0.04	1.0 ± 1.2	$p = 0.43$
Mφ	1.8 ± 0.6	2.2 ± 0.8	$p = 0.45$
Resident monocytes	0.4 ± 0.1	0.4 ± 0.1	$p = 0.96$
Inflammatory monocytes	0.2 ± 0.03	0.2 ± 0.2	$p = 0.82$

Data are percentages unless otherwise indicated.

(16). In our study, mRNA expression of *Inam* in these tissues was clearly absent in the *Inam*-null mouse (Fig. 1D). To assess the induction of *Inam* mRNA expression in response to TLR agonists in vivo, we performed qPCR analysis using spleens at 3 h after i.p. administration of those agonists or PBS. The levels of *Inam* mRNA expression was strongly induced by polyI:C, but not other TLR agonists (Fig. 1E). Hence, these data indicate that polyI:C is the strongest TLR agonist to induce *Inam* expression of the TLR agonists tested in vivo. To investigate the cellular distribution of INAM protein expression, we performed flow cytometric analysis using polyclonal Abs to mouse INAM after i.p. administration of polyI:C. The levels of INAM protein expression in these cells clearly reflected the absence of the mRNA (Fig. 1F). Flow cytometric analysis of spleen cells demonstrated that INAM expression was induced in all myeloid lineage cells, including DC subsets and NK cells. In particular, INAM expression was highly induced in pDCs and F4/80$^+$ Mφs.

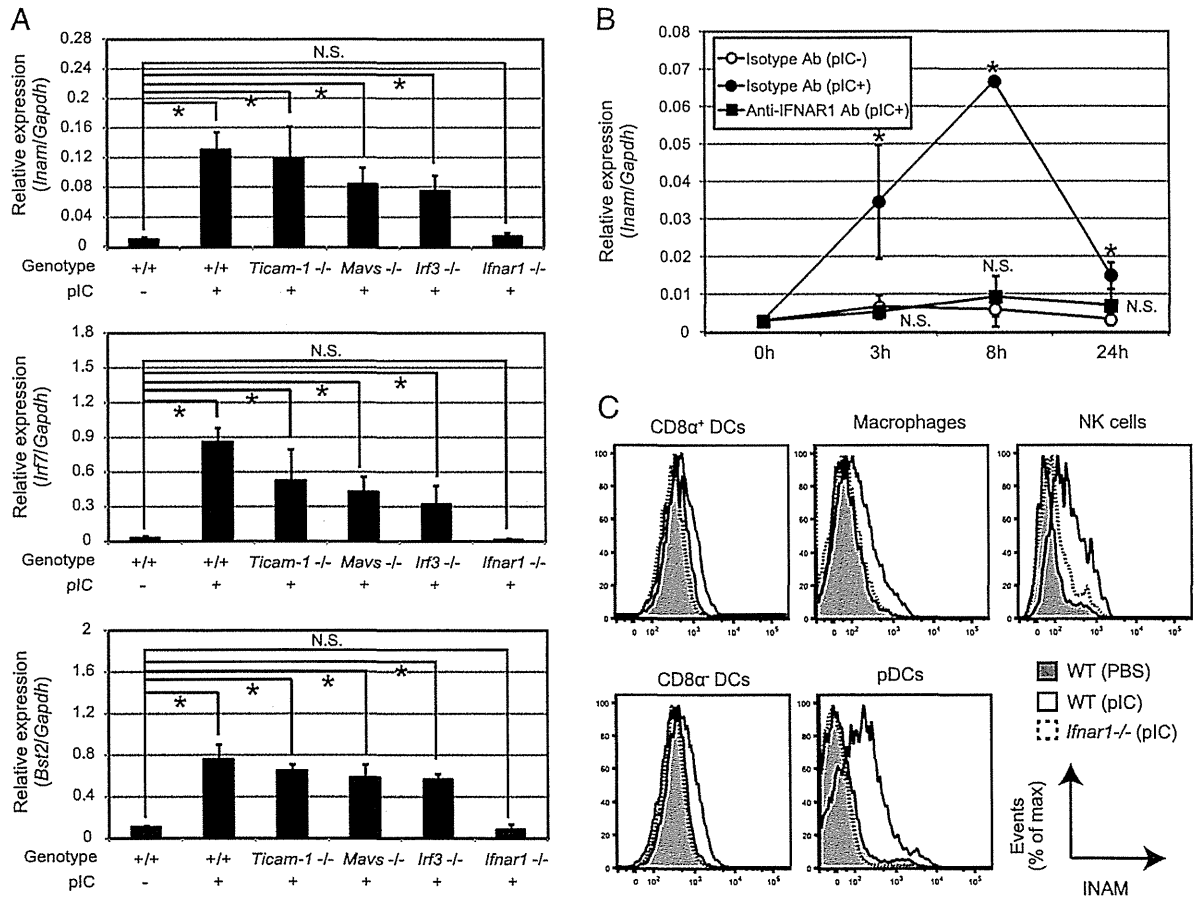

FIGURE 2. Signaling pathway of INAM induction in vivo. (**A**) *Inam* expression in splenocytes derived from various gene-manipulated mice. After 3 h, total RNA were isolated from the spleens of mice in each group ($n = 3$) and subjected to quantitative PCR to determine *Inam*, *Irf7*, and *Bst2* expression. (**B**) Type I IFN signaling is required for *Inam* expression of splenocytes derived from WT mice. Splenocytes ($n = 3$) were treated with polyI:C (pIC), IFNAR1-blocking Ab, or isotype control Ab for 0, 3, 8, and 24 h. (**C**) Type I IFN signaling is required for INAM expression of DC subsets, NK cells, and Mφs. WT and *Ifnar1*$^{-/-}$ mice were i.p. injected with 200 μg polyI:C or PBS ($n = 2$). After 12 h, INAM expression of each immune cell type was analyzed by flow cytometry. The data shown are representative of at least two independent experiments. Data are means ± SD of three independent samples. *$p < 0.05$.

Type I IFN signaling is required for INAM induction in vivo

The TLR3/TICAM-1 and MDA5/mitochondrial antiviral signaling protein pathways activate the transcription factor IRF3 in response to viral RNA. In BMDC, polyI:C (an analog of virus dsRNA) directly induces INAM expression via the TICAM-1/IRF3 pathway (16). Moreover, in the absence of pattern recognition receptor signals, IFN-α stimulation triggers INAM expression in BMDC. However, it is unclear which innate signal is required for its up-regulation in vivo. To understand the inducible pathway of *Inam* expression, we investigated its expression in spleen cells derived from various genetically manipulated mice. After polyI:C stimulation, *Inam* expression was completely undetectable in IFN (α and β) receptor 1 $(Ifnar1)^{-/-}$ mice, but not in $Ticam\text{-}1^{-/-}$ mice, a similar pattern of expression to that seen in type I IFN–inducible genes including *Irf7* and *Bst2* (Fig. 2A). Additionally, *Inam* expression was partially reduced in mice deficient in *Mavs* or *Irf3*, factors that are critical for producing type I IFN in response to polyI:C (3, 16). To assess the effect of type I IFN in WT mice, splenocytes were stimulated with polyI:C in the presence of anti-IFNAR1 Ab or isotype control Ab. Expression of *Inam* was transient, peaking at 8 h in the stimulated group in the presence of isotype control Ab (Fig. 2B). In contrast, blocking of the type I IFN receptor led to abrogation of *Inam* induction. In agreement with these results, INAM protein expression was completely undetectable in DC subsets, NK cells, and Mφs derived from IFNAR1-deficient mice (Fig. 2C). Hence, these data indicate that INAM expression depends on the IFNAR1 signaling pathway in vivo.

INAM is required for IFN-γ production through NK–accessory interaction

To identify the accessory cells directly responding to polyI:C and leading to IFN-γ production from NK cells, we performed an experiment on a coculture consisting of MACS-sorted splenic NK cells and myeloid immune cells including DC subsets and Mφs. Purified NK cells cultured in medium with or without polyI:C did not produce IFN-γ (Fig. 3A). In contrast, a high level of IFN-γ production was observed in the supernatant of NK cells cocultured with $CD8\alpha^+$ cDCs and Mφs in the presence of polyI:C, but not in pDCs and $CD8\alpha^-$ cDCs. In our reports, cell-to-cell contact is required for the interaction between NK cells and BMDC (8, 16). To confirm that the cell-to-cell contact is a prerequisite for the interaction between NK cells and splenic accessory cells, we performed coculture experiments using transwell system. As

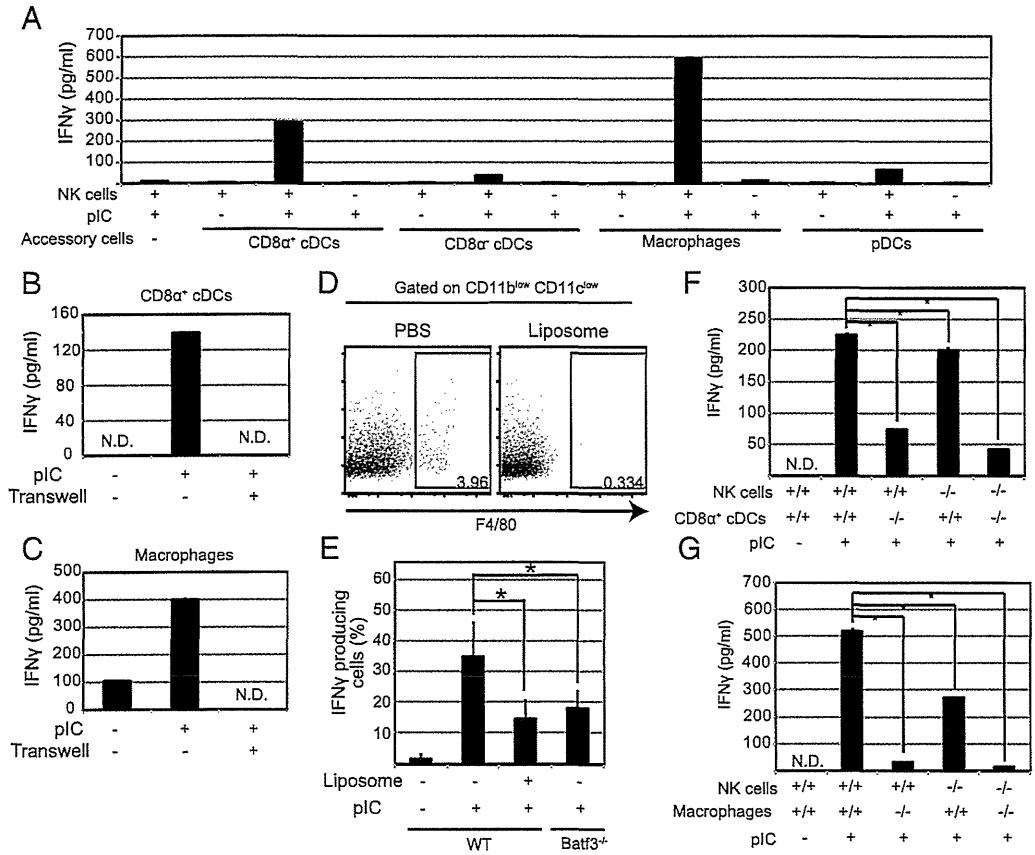

FIGURE 3. INAM-dependent NK cell activation in vitro. (**A**) IFN-γ production of NK cells via polyI:C (pIC)-stimulated DC subsets and Mφs. NK cells, DC subsets, and Mφs were enriched by MACS separation from WT and $Inam^{-/-}$ mice. (**B**) Cell-to-cell contact-dependent NK cell activation via $CD8\alpha^+$ cDCs. (**C**) Cell-to-cell contact-dependent NK cell activation via Mφs. NK cells were cocultured with DC subsets and Mφs in the presence of polyI:C (20 μg/ml) for 24 h. The concentrations of IFN-γ in the culture supernatants were measured by ELISA. (**D**) Mφ depletion with clodronate liposomes. WT mice were i.p. injected with clodronate liposomes (150 μl/mouse) to remove Mφs. After 24 h, the efficiency of Mφ depletion was measured by FACS analysis. (**E**) Production of IFN-γ by NK cells in WT, Mφ-depleted WT, and $Batf3^{-/-}$ mice. WT, Mφ-depleted WT, and $Batf3^{-/-}$ mice were i.p. injected with 200 μg polyI:C ($n = 3$). After 3 h, splenocytes were isolated, cultured with brefeldin A for an additional 4 h, and analyzed for intracellular content of IFN-γ by FACS, gating on $CD3\varepsilon^-/NK1.1^+$ cells. (**F**) INAM-dependent NK cell activation via $CD8\alpha^+$ cDCs. (**G**) INAM-dependent NK cell activation via Mφs. NK cells, $CD8\alpha^+$ cDCs, and Mφs were enriched via MACS separation from WT and $Inam^{-/-}$ mice. NK cells were cocultured with $CD8\alpha^+$ cDCs or Mφs in the presence of polyI:C (20 μg/ml) for 24 h. The concentrations of IFN-γ in the culture supernatants were measured by ELISA. The data shown are representative of at least two independent experiments. Data are means ± SD of three independent samples. $*p < 0.05$.

a result, IFN-γ production was completely blocked under transwell conditions (Fig. 3B, 3C). Therefore, NK cells are primed through contact with CD8α$^+$ cDCs and Mφs independent of soluble mediators. To directly test the contribution of CD8α$^+$ cDCs and Mφs to polyI:C-mediated NK cell activation in vivo, we analyzed *Batf3*$^{-/-}$ mice, which largely lack the CD8α$^+$ cDC population in the spleen of C57BL/6 mice (21), and Mφ-depleted mice generated by clodronate liposome injection (22, 23). Approximately 85% of Mφs were depleted at 24 h after clodronate liposome injection (Fig. 3D). Three hours after polyI:C stimulation, NK cell secretion of IFN-γ was partially decreased in *Batf3*$^{-/-}$ and Mφ-depleted mice (Fig. 3E). These results indicate that CD8α$^+$ cDCs and Mφs are responsible for secretion of IFN-γ from NK cells in response to polyI:C stimulation.

INAM acts on NK cells and BMDC to orchestrate NK–DC interaction triggered by polyI:C stimulation (16). To investigate the role of INAM in the interaction of NK-CD8α$^+$ cDC and NK-Mφ, we performed an experiment on a coculture of MACS-sorted splenic NK cells with their accessory cells isolated from WT and *Inam*$^{-/-}$ mice. Cocultures of NK cells and accessory cells lacking INAM showed that IFN-γ production from NK cells required INAM expression in either NK cells or accessory cells (Fig. 3F, 3G). Notably, deficiency of INAM in both NK and accessory cells led to a marked decrease in IFN-γ production. Taken together, these results suggest that INAM is required for cell–cell contact in both NK cells and accessory cells and early IFN-γ production by NK cells.

INAM plays a critical role in rapid IFN-γ production by NK cells in response to polyI:C in vivo

To investigate the role of INAM in polyI:C-mediated cytotoxicity of NK cells, we injected WT and *Inam*$^{-/-}$ mice with polyI:C. After 0, 3, and 24 h, we isolated splenic NK cells and measured cytotoxicity ex vivo. In the four NK-sensitive cell lines B16D8, RMA-S, B16F10, and YAC-1, we found no difference between WT and *Inam*$^{-/-}$ mice in the cytotoxic effect of NK cells against these cell lines (data not shown). Consistent with these results, cell numbers expressing granzyme B, known as a cytotoxic lymphocyte protease, barely differed between splenocytes of WT and *Inam*$^{-/-}$ mice (Fig. 4A). To determine the role of INAM in NK cell production of IFN-γ in response to polyI:C, we isolated splenocytes 0, 1, and 3 h after injecting WT and *Inam*$^{-/-}$ mice with polyI:C and determined the intracellular content of IFN-γ in NK cells. After 3 h, NK cells isolated from *Inam*$^{-/-}$ mice produced less IFN-γ than WT NK cells (Fig. 4B). Additionally, we also measured the numbers of other cytokine-producing cells, including GM-CSF, IL-2, and TNF-α, from NK cells at 3 h after polyI:C stimulation in WT and *Inam*$^{-/-}$ mice and confirmed no INAM dependence of the production of these cytokines (Supplemental Fig. 2A). Therefore, INAM specifically regulates IFN-γ through CD8α DC at least within this time frame. We also measured CD69 expression, known as an NK-activating marker at 0, 3, and 24 h after polyI:C stimulation. CD69 upregulation in response to polyI:C was partially impaired in NK cells from *Inam*$^{-/-}$ mice in comparison with those from WT mice 24 h after polyI:C stimulation (Fig. 4C). We found no clear difference between WT and *Inam*$^{-/-}$ mice in expression of CD27 or NK1.1, both of which evoke IFN-γ production through their interaction with the ligands, or in any other NK receptors at 0, 3, and 24 h after polyI:C injection (24) (Supplemental Fig. 1B). These results indicate that INAM-mediated NK activation is independent of incremental expression of these receptors. Previous reports suggested that proinflammatory cytokines including IL-12, IL-15, IL-18, and type I IFN play critical roles in the cytotoxicity and IFN-γ production of NK cells (15, 25, 26). To determine their expression at 0, 3, and 24 h

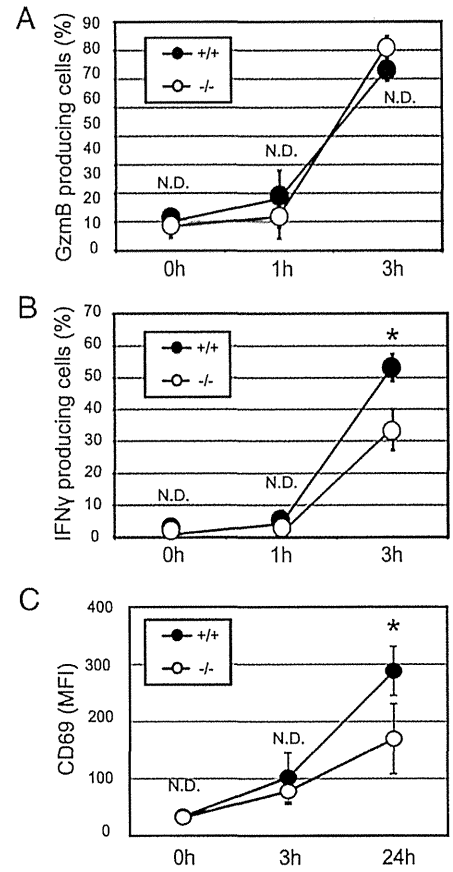

FIGURE 4. INAM-dependent NK cell activation in vivo. (**A**) Production of granzyme B (GzmB) by NK cells. (**B**) Production of IFN-γ by NK cells. WT (+/+) and *Inam*$^{-/-}$ (−/−) mice were i.p. injected with 200 μg polyI:C. After 0, 1, and 3 h, splenocytes were isolated, cultured with brefeldin A for an additional 4 h, and analyzed for intracellular content of IFN-γ and granzyme B by FACS, gating on CD3ε$^-$/NK1.1$^+$ cells (n = 3 or 4). (**C**) Expression of CD69 on the surface of NK cells. WT (+/+) and *Inam*$^{-/-}$ (−/−) mice were i.p. injected with 200 μg polyI:C or PBS. After 0, 3, and 24 h, CD69 expression was assayed by FACS, and the data were quantitatively analyzed using mean fluorescence intensity (MFI), gating on CD3ε$^-$/NK1.1$^+$ cells (n = 3). The data shown are representative of at least two independent experiments. Data are means ± SD of three independent samples. *$p < 0.05$.

after polyI:C stimulation, we performed ELISA and qPCR analysis of serum and spleen cells from WT and *Inam*$^{-/-}$ mice. However, protein levels of IL12p40, IFN-α, and IFN-β were not affected by *Inam* disruption in mice (Supplemental Fig. 2B). Additionally, mRNA expression of *Il-15* and *Il-18* genes was not decreased in *Inam*$^{-/-}$ mice (Supplemental Fig. 2C). These results suggest that INAM plays a critical role in the CD69 expression and rapid IFN-γ production, but not the cytotoxicity, of NK cells in response to polyI:C in a cytokine-independent manner.

INAM is required for the antimetastatic effect by polyI:C-based cancer immunotherapy

Malignant melanomas are one of the most important targets of NK-mediated cancer immunotherapy (27). In this study, we tested two types of polyI:C-based cancer immunotherapy model using B16D8 and B16F10 cell lines. NK cells show high cytotoxicity activity against B16D8 cells established in our laboratory as a subline of the B16 melanoma cell line (28). This subline was characterized by its low or virtually absent metastatic properties when injected s.c. into syngeneic C57BL/6 mice. In contrast, the B16F10 subline was characterized by its high metastatic capacity

especially into the lung (29). In this model, NK1.1$^+$ cells and IFN-γ have a critical role in the suppression of pulmonary metastases (30).

A mouse model with s.c.-implanted B16D8 and polyI:C therapy has been established in our laboratory (8). To investigate the function of INAM involved in tumor growth retardation mediated by polyI:C, we challenged WT and *Inam*$^{-/-}$ mice with B16D8 implantation and then treated the mice with i.p. injection of polyI:C. The rate of B16D8 growth retardation was indistinguishable between WT and *Inam*$^{-/-}$ mice (Supplemental Fig. 3), which was largely dependent on the antitumor effect of polyI:C. This result is consistent with the observation that there is no difference in tumoricidal activity against B16D8 between WT and *Inam*$^{-/-}$ mice. To determine the role of INAM in the production of IFN-γ by lung NK cells in response to polyI:C, we isolated leukocytes from the lung at 0, 3, and 6 h after administration of polyI:C to B16F10-injected WT and *Inam*$^{-/-}$ mice and determined the intracellular content of IFN-γ in NK cells (Fig. 5A). After 6 h, NK cells isolated from *Inam*$^{-/-}$ mice produced less IFN-γ than WT NK cells (Fig. 5B). To investigate the function of INAM involved in pulmonary metastases induced by polyI:C, we i.v. challenged WT and *Inam*$^{-/-}$ mice with B16F10 cells and then treated the mice by i.p. injection of polyI:C. After four rounds of polyI:C treatment, we counted tumor foci in the lung. Under unstimulated conditions, there was no difference in the number and size of tumor foci in the lungs between WT and *Inam*$^{-/-}$ mice (Fig. 5C). In WT mice, i.p. injection of polyI:C exerted a significant inhibition in the growth of pulmonary metastases in tumor-bearing mice compared with PBS controls (Fig. 5D). In contrast, the effect of polyI:C therapy for pulmonary metastases was partially abrogated in *Inam*$^{-/-}$ mice. These results demonstrate that INAM plays a critical role in IFN-γ production by lung NK cells in response to polyI:C and unequivocally exhibits antitumor function in polyI:C-based cancer immunotherapy against IFN-γ–sensitive tumors metastasized to the lung.

BMDC confer direct cytotoxic activity on NK cells by stimulation with RNA via INAM-dependent cell–cell contact (16). Then, NK cells kill tumor cells via effectors, such as TRAIL and granzyme B, secondary to upregulation of INAM. However, splenic DCs hardly induce direct NK cytotoxicity as shown in this study. In this study, *Inam*$^{-/-}$ mice studies revealed that DC/Mφ primed NK cells in vivo to induce IFN-γ that was a major effector for NK antimetastatic activity. Thus, taken together with the previous results that BMDCs induce NK cytotoxicity via INAM (16), INAM-involved DC–NK contact induces two arrays of NK tumoricidal activities, killer effector and IFN-γ producer, depending on the properties of DC subsets. The role of INAM in ILC activation will be a matter of future interest in this context.

Discussion

In this study, we provide the first demonstration, to our knowledge, that INAM plays a critical role in the interactions of NK-CD8α$^+$ cDCs and Mφs leading to IFN-γ production from NK cells in vivo. Additionally, we also propose that INAM is a novel target molecule for cancer immunotherapy against IFN-γ–suppressible metastasis.

IFN-γ coordinates a diverse array of cellular programs via STAT1 activation, such as antimicrobial response, anti- or protumor response, production of proinflammatory cytokines, and induction of IRF1 (31). IRF1 activates a large number of secondary response genes, which carry out a range of immunomodulatory functions (32, 33). In secondary lymphoid organs including spleen and lymph nodes, NK cells are a dominant IFN-γ producer responding to polyI:C (5). IFN-γ primes Ag-specific CD4$^+$ and CD8$^+$ T cells and also activates other innate immune cells including Mφs (34–36). The TLR3-dependent IFN-γ signaling pathway is important in protecting the host from pathogenesis induced by Coxsackievirus group B serotype 3 infection, which leads to IFN-γ production from NK cells (37, 38). Hence, IFN-γ

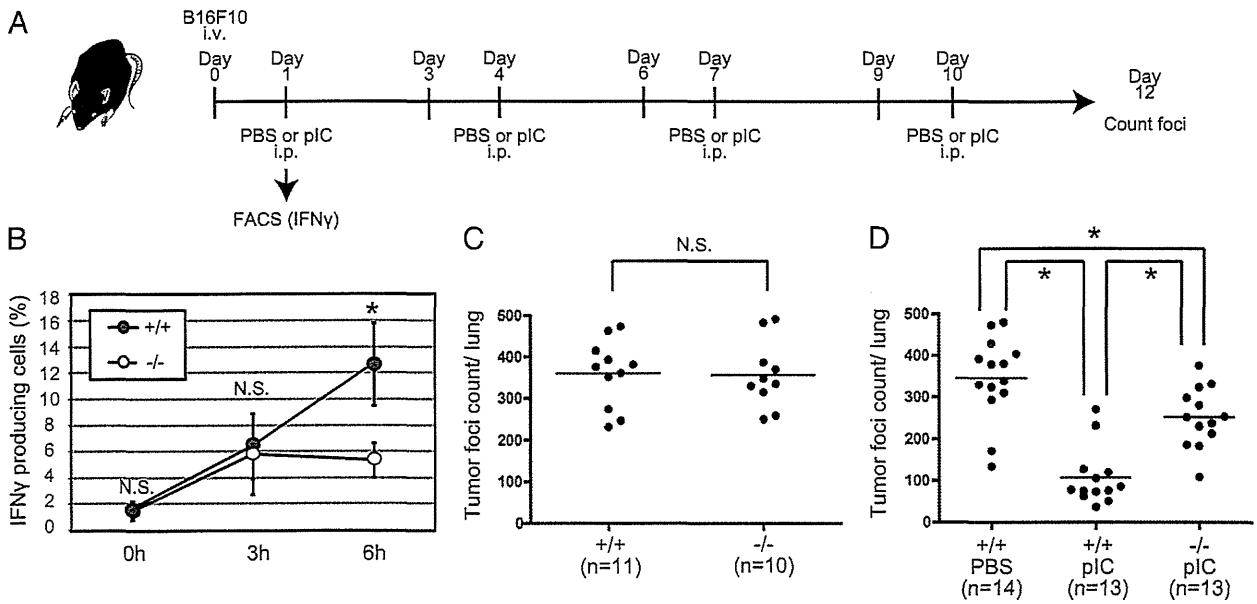

FIGURE 5. Antimetastatic activity of INAM against B16F10 melanoma. (**A**) The time schedule of polyI:C (pIC) treatment. (**B**) Production of IFN-γ by NK cells in the lung. After 24 h, WT and *Inam*$^{-/-}$ mice were i.p. injected with 200 μg polyI:C. Lung leukocytes were isolated and cultured with brefeldin A for an additional 4 h, and analyzed for frequency of NK cells and production of IFN-γ/granzyme B by FACS, gating on CD3ε$^-$/NK1.1$^+$ cells (n = 3 or 4). (**C**) Tumor foci counts in the lung of WT (+/+) and *Inam*$^{-/-}$ (−/−) mice under unstimulated conditions at day 12. (**D**) Tumor foci in the lung of WT (+/+) and *Inam*$^{-/-}$ (−/−) mice. WT (+/+) and *Inam*$^{-/-}$ (−/−) mice were i.v. injected with 2 × 10^5 B16F10 melanoma cells at day 0. At days 1, 4, 7, and 10, WT and *Inam*$^{-/-}$ mice were i.p. injected with 200 μg polyI:C. At day 12, the mice were sacrificed, and lungs were removed and fixed in 10% formalin solution to count surface colonies under a dissection microscope. The data shown are representative of at least two independent experiments. Data are means ± SD of three independent samples. *$p < 0.05$.

derived from NK cells controls innate and adaptive immunity, leading to a Th1 response.

In this study, we show that INAM evokes IFN-γ production by NK cells in the early phase by polyI:C stimulation (Figs. 4B, 5B). In a murine CMV infection model, IFN-γ is induced in NK cells by IL-12 and IL-18 produced by murine CMV–infected CD11b$^+$ cDCs, whereas these cytokines barely evoke any cytotoxic response in NK cells (39). In addition, IFN-γ production from NK cells is induced by anti-CD27 Ab stimulation, but again no cytotoxic response is triggered (24). Therefore, these reports indicate that NK cell cytotoxicity and IFN-γ production are independently controlled by different mechanisms. We found no clear difference between WT and *Inam*$^{-/-}$ mice in expression of these cell surface molecules and cytokines. Hence, the INAM-dependent IFN-γ production from NK cells is based on an as-yet-unknown mechanism(s) acting in a manner independent of these molecules.

CpG DNA is known to induce IFN-γ from NK cells, which is mediated through pDCs. TLR9 in pDCs responds to CpG, and the pDCs liberate IFN-α and TNF-α that participate in the induction of IFN-γ from NK cells (40). We checked induction of the Inam mRNA in spleen after stimulation with CpG in WT and *Inam*$^{-/-}$ mice (Fig. 1E). The levels of *Inam* mRNA as well as numbers of IFN-γ–producing cells were hardly increased in response to i.p. administration of CpG in WT as well as *Inam*$^{-/-}$ mice, suggesting no participation of INAM in CpG-induced NK cell IFN-γ production (data not shown). CpG participates in the activation of the TLR9 pathway in pDCs, but INAM in splenic cDCs and Mφs does not participate in CpG-mediated NK priming. The result is consistent with the fact that polyI:C is an agonist for TLR3 (but not for TLR9 predominantly expressed in pDCs), which is mainly expressed in CD8α$^+$ DCs, especially professional Ag-presenting CD141$^+$ and CD103$^+$ DCs in mice (41).

CD8α$^+$ cDCs directly recognize polyI:C via the TLR3/TICAM-1 pathway and promote IFN-γ production from NK cells in vitro (9). However, previous analysis of *Batf3*$^{-/-}$ mice indicated that absence of CD8α$^+$ cDCs resulted in weak NK cell activation, in agreement with our data (19). We also found that NK cell secretion of IFN-γ was partially decreased in mice depleted of Mφs by injection of clodronate liposomes (Fig. 3E). Notably, expression of INAM by both NK cells and accessory cells is required for early IFN-γ production through NK-CD8α$^+$ cDC and/or NK–Mφ interactions (Fig. 3F, 3G). The physiological role of these accessory cells in NK activation is poorly understood. However, our results indicate that CD8α$^+$ cDCs and Mφs facilitate early secretion of IFN-γ from NK cells in response to polyI:C and INAM plays a critical role in the interaction between NK cells and CD8α$^+$ cDCs and/or Mφs, leading to IFN-γ production.

IFN-γ exhibits both anti- and protumor activities (42). Systemic administration of polyI:C exerted a significant inhibitory effect on the growth of lung metastases in B16F10 melanoma-bearing mice (30, 42). Using this model, a previous study reported that NK1.1$^+$ cells and IFN-γ have a critical role in the protection of lung metastases (30). Previous studies demonstrated that the IFN-γ receptor expressed on host cells, but not on melanoma cells, is important for development of lung metastases (43–45). Hence, lung metastases are prevented by the IFN-γ–inducible immune response following NK cell activation. We show that INAM is involved in the IFN-γ production of lung NK cells in response to polyI:C stimulation and unequivocally exhibits antitumor functions in polyI:C-based cancer immunotherapy against IFN-γ–sensitive tumor foci in the lung (Fig. 5D). Therefore, we propose that INAM is a novel target molecule for cancer immunotherapy against IFN-γ–suppressible metastasis.

Acknowledgments

We thank the members in Seya Laboratory (Hokkaido University). Tumor implant studies were supported by A. Morii-Sakai (Seya Laboratory). Thoughtful discussions with Dr. T. Taniguchi (University of Tokyo) are gratefully acknowledged.

Disclosures

The authors have no financial conflicts of interest.

References

1. Seya, T., J. Kasamatsu, M. Azuma, H. Shime, and M. Matsumoto. 2011. Natural killer cell activation secondary to innate pattern sensing. *J. Innate Immun.* 3: 264–273.
2. Reed, S. G., M. T. Orr, and C. B. Fox. 2013. Key roles of adjuvants in modern vaccines. *Nat. Med.* 19: 1597–1608.
3. Kumar, H., S. Koyama, K. J. Ishii, T. Kawai, and S. Akira. 2008. Cutting edge: cooperation of IPS-1- and TRIF-dependent pathways in poly IC-enhanced antibody production and cytotoxic T cell responses. *J. Immunol.* 180: 683–687.
4. Trumpfheller, C., M. Caskey, G. Nchinda, M. P. Longhi, O. Mizenina, Y. Huang, S. J. Schlesinger, M. Colonna, and R. M. Steinman. 2008. The microbial mimic poly IC induces durable and protective CD4$^+$ T cell immunity together with a dendritic cell targeted vaccine. *Proc. Natl. Acad. Sci. USA* 105: 2574–2579.
5. Longhi, M. P., C. Trumpfheller, J. Idoyaga, M. Caskey, I. Matos, C. Kluger, A. M. Salazar, M. Colonna, and R. M. Steinman. 2009. Dendritic cells require a systemic type I interferon response to mature and induce CD4+ Th1 immunity with poly IC as adjuvant. *J. Exp. Med.* 206: 1589–1602.
6. Talmadge, J. E., J. Adams, H. Phillips, M. Collins, B. Lenz, M. Schneider, E. Schlick, R. Ruffmann, R. H. Wiltrout, and M. A. Chirigos. 1985. Immunomodulatory effects in mice of polyinosinic-polycytidylic acid complexed with poly-L-lysine and carboxymethylcellulose. *Cancer Res.* 45: 1058–1065.
7. Spits, H., D. Artis, M. Colonna, A. Diefenbach, J. P. Di Santo, G. Eberl, S. Koyasu, R. M. Locksley, A. N. McKenzie, R. E. Mebius, et al. 2013. Innate lymphoid cells—a proposal for uniform nomenclature. *Nat. Rev. Immunol.* 13: 145–149.
8. Akazawa, T., T. Ebihara, M. Okuno, Y. Okuda, M. Shingai, K. Tsujimura, T. Takahashi, M. Ikawa, M. Okabe, N. Inoue, et al. 2007. Antitumor NK activation induced by the Toll-like receptor 3-TICAM-1 (TRIF) pathway in myeloid dendritic cells. *Proc. Natl. Acad. Sci. USA* 104: 252–257.
9. Miyake, T., Y. Kumagai, H. Kato, Z. Guo, K. Matsushita, T. Satoh, T. Kawagoe, H. Kumar, M. H. Jang, T. Kawai, et al. 2009. Poly I:C-induced activation of NK cells by CD8 alpha+ dendritic cells via the IPS-1 and TRIF-dependent pathways. *J. Immunol.* 183: 2522–2528.
10. Wulff, S., R. Pries, and B. Wollenberg. 2010. Cytokine release of human NK cells solely triggered with Poly I:C. *Cell. Immunol.* 263: 135–137.
11. Fuchs, A., W. Vermi, J. S. Lee, S. Lonardi, S. Gilfillan, R. D. Newberry, M. Cella, and M. Colonna. 2013. Intraepithelial type 1 innate lymphoid cells are a unique subset of IL-12- and IL-15-responsive IFN-γ-producing cells. *Immunity* 38: 769–781.
12. Matsumoto, M., K. Funami, H. Oshiumi, and T. Seya. 2013. Toll-IL-1-receptor-containing adaptor molecule-1: a signaling adaptor linking innate immunity to adaptive immunity. *Prog. Mol. Biol. Transl. Sci.* 117: 487–510.
13. Shime, H., A. Kojima, A. Maruyama, Y. Saito, H. Oshiumi, M. Matsumoto, and T. Seya. 2014. Myeloid-derived suppressor cells confer tumor-suppressive functions on natural killer cells via polyinosinic:polycytidylic acid treatment in mouse tumor models. *J. Innate Immun.* 6: 293–305.
14. Tu, Z., A. Bozorgzadeh, R. H. Pierce, J. Kurtis, I. N. Crispe, and M. S. Orloff. 2008. TLR-dependent cross talk between human Kupffer cells and NK cells. *J. Exp. Med.* 205: 233–244.
15. Lucas, M., W. Schachterle, K. Oberle, P. Aichele, and A. Diefenbach. 2007. Dendritic cells prime natural killer cells by trans-presenting interleukin 15. *Immunity* 26: 503–517.
16. Ebihara, T., M. Azuma, H. Oshiumi, J. Kasamatsu, K. Iwabuchi, K. Matsumoto, H. Saito, T. Taniguchi, M. Matsumoto, and T. Seya. 2010. Identification of a polyI:C-inducible membrane protein that participates in dendritic cell-mediated natural killer cell activation. *J. Exp. Med.* 207: 2675–2687.
17. Sato, M., H. Sucmori, N. Hata, M. Asagiri, K. Ogasawara, K. Nakao, T. Nakaya, M. Katsuki, S. Noguchi, N. Tanaka, and T. Taniguchi. 2000. Distinct and essential roles of transcription factors IRF-3 and IRF-7 in response to viruses for IFN-alpha/beta gene induction. *Immunity* 13: 539–548.
18. Takaki, H., M. Takeda, M. Tahara, M. Shingai, H. Oshiumi, M. Matsumoto, and T. Seya. 2013. The MyD88 pathway in plasmacytoid and CD4+ dendritic cells primarily triggers type I IFN production against measles virus in a mouse infection model. *J. Immunol.* 191: 4740–4747.
19. McCartney, S., W. Vermi, S. Gilfillan, M. Cella, T. L. Murphy, R. D. Schreiber, K. M. Murphy, and M. Colonna. 2009. Distinct and complementary functions of MDA5 and TLR3 in poly(I:C)-mediated activation of mouse NK cells. *J. Exp. Med.* 206: 2967–2976.
20. Hayakawa, Y., N. D. Huntington, S. L. Nutt, and M. J. Smyth. 2006. Functional subsets of mouse natural killer cells. *Immunol. Rev.* 214: 47–55.
21. Edelson, B. T., T. R. Bradstreet, W. Kc, K. Hildner, J. W. Herzog, J. Sim, J. H. Russell, T. L. Murphy, E. R. Unanue, and K. M. Murphy. 2011. Batf3-dependent CD11b(low/-) peripheral dendritic cells are GM-CSF-independent

and are not required for Th cell priming after subcutaneous immunization. *PLoS ONE* 6: e25660.
22. Hildner, K., B. T. Edelson, W. E. Purtha, M. Diamond, H. Matsushita, M. Kohyama, B. Calderon, B. U. Schraml, E. R. Unanue, M. S. Diamond, et al. 2008. Batf3 deficiency reveals a critical role for CD8alpha$^+$ dendritic cells in cytotoxic T cell immunity. *Science* 322: 1097–1100.
23. Tussiwand, R., W. L. Lee, T. L. Murphy, M. Mashayekhi, W. Kc, J. C. Albring, A. T. Satpathy, J. A. Rotondo, B. T. Edelson, N. M. Kretzer, et al. 2012. Compensatory dendritic cell development mediated by BATF-IRF interactions. *Nature* 490: 502–507.
24. Takeda, K., H. Oshima, Y. Hayakawa, H. Akiba, M. Atsuta, T. Kobata, K. Kobayashi, M. Ito, H. Yagita, and K. Okumura. 2000. CD27-mediated activation of murine NK cells. *J. Immunol.* 164: 1741–1745.
25. Ferlazzo, G., M. Pack, D. Thomas, C. Paludan, D. Schmid, T. Strowig, G. Bougras, W. A. Muller, L. Moretta, and C. Münz. 2004. Distinct roles of IL-12 and IL-15 in human natural killer cell activation by dendritic cells from secondary lymphoid organs. *Proc. Natl. Acad. Sci. USA* 101: 16606–16611.
26. Takeda, K., H. Tsutsui, T. Yoshimoto, O. Adachi, N. Yoshida, T. Kishimoto, H. Okamura, K. Nakanishi, and S. Akira. 1998. Defective NK cell activity and Th1 response in IL-18-deficient mice. *Immunity* 8: 383–390.
27. Burke, S., T. Lakshmikanth, F. Colucci, and E. Carbone. 2010. New views on natural killer cell-based immunotherapy for melanoma treatment. *Trends Immunol.* 31: 339–345.
28. Tanaka, H., Y. Mori, H. Ishii, and H. Akedo. 1988. Enhancement of metastatic capacity of fibroblast-tumor cell interaction in mice. *Cancer Res.* 48: 1456–1459.
29. Brown, L. M., D. R. Welch, and S. R. Rannels. 2002. B16F10 melanoma cell colonization of mouse lung is enhanced by partial pneumonectomy. *Clin. Exp. Metastasis* 19: 369–376.
30. Jiang, Q., H. Wei, and Z. Tian. 2008. IFN-producing killer dendritic cells contribute to the inhibitory effect of poly I:C on the progression of murine melanoma. *J. Immunother.* 31: 555–562.
31. Schroder, K., P. J. Hertzog, T. Ravasi, and D. A. Hume. 2004. Interferon-gamma: an overview of signals, mechanisms and functions. *J. Leukoc. Biol.* 75: 163–189.
32. Honda, K., and T. Taniguchi. 2006. IRFs: master regulators of signalling by Toll-like receptors and cytosolic pattern-recognition receptors. *Nat. Rev. Immunol.* 6: 644–658.
33. Miyamoto, M., T. Fujita, Y. Kimura, M. Maruyama, H. Harada, Y. Sudo, T. Miyata, and T. Taniguchi. 1988. Regulated expression of a gene encoding a nuclear factor, IRF-1, that specifically binds to IFN-beta gene regulatory elements. *Cell* 54: 903–913.
34. O'Sullivan, T., R. Saddawi-Konefka, W. Vermi, C. M. Koebel, C. Arthur, J. M. White, R. Uppaluri, D. M. Andrews, S. F. Ngiow, M. W. L. Teng, et al. 2012. Cancer immunoediting by the innate immune system in the absence of adaptive immunity. *J. Exp. Med.* 209: 1869–1882.
35. Mailliard, R. B., Y. I. Son, R. Redlinger, P. T. Coates, A. Giermasz, P. A. Morel, W. J. Storkus, and P. Kalinski. 2003. Dendritic cells mediate NK cell help for Th1 and CTL responses: two-signal requirement for the induction of NK cell helper function. *J. Immunol.* 171: 2366–2373.
36. Martín-Fontecha, A., L. L. Thomsen, S. Brett, C. Gerard, M. Lipp, A. Lanzavecchia, and F. Sallusto. 2004. Induced recruitment of NK cells to lymph nodes provides IFN-gamma for T(H)1 priming. *Nat. Immunol.* 5: 1260–1265.
37. Hühn, M. H., M. Hultcrantz, K. Lind, H. G. Ljunggren, K. J. Malmberg, and M. Flodström-Tullberg. 2008. IFN-gamma production dominates the early human natural killer cell response to Coxsackievirus infection. *Cell. Microbiol.* 10: 426–436.
38. Negishi, H., T. Osawa, K. Ogami, X. Ouyang, S. Sakaguchi, R. Koshiba, H. Yanai, Y. Seko, H. Shitara, K. Bishop, et al. 2008. A critical link between Toll-like receptor 3 and type II interferon signaling pathways in antiviral innate immunity. *Proc. Natl. Acad. Sci. USA* 105: 20446–20451.
39. Andoniou, C. E., S. L. H. van Dommelen, V. Voigt, D. M. Andrews, G. Brizard, C. Asselin-Paturel, T. Delale, K. J. Stacey, G. Trinchieri, and M. A. Degli-Esposti. 2005. Interaction between conventional dendritic cells and natural killer cells is integral to the activation of effective antiviral immunity. *Nat. Immunol.* 6: 1011–1019.
40. Marshall, J. D., D. S. Heeke, C. Abbate, P. Yee, and G. Van Nest. 2006. Induction of interferon-gamma from natural killer cells by immunostimulatory CpG DNA is mediated through plasmacytoid-dendritic-cell-produced interferon-alpha and tumour necrosis factor-alpha. *Immunology* 117: 38–46.
41. Jongbloed, S. L., A. J. Kassianos, K. J. McDonald, G. J. Clark, X. Ju, C. E. Angel, C. J. Chen, P. R. Dunbar, R. B. Wadley, V. Jeet, et al. 2010. Human CD141+ (BDCA-3)+ dendritic cells (DCs) represent a unique myeloid DC subset that cross-presents necrotic cell antigens. *J. Exp. Med.* 207: 1247–1260.
42. Zaidi, M. R., and G. Merlino. 2011. The two faces of interferon-γ in cancer. *Clin. Cancer Res.* 17: 6118–6124.
43. Forte, G., A. Rega, S. Morello, A. Luciano, C. Arra, A. Pinto, and R. Sorrentino. 2012. Polyinosinic-polycytidylic acid limits tumor outgrowth in a mouse model of metastatic lung cancer. *J. Immunol.* 188: 5357–5364.
44. Takeda, K., M. Nakayama, M. Sakaki, Y. Hayakawa, M. Imawari, K. Ogasawara, K. Okumura, and M. J. Smyth. 2011. IFN-γ production by lung NK cells is critical for the natural resistance to pulmonary metastasis of B16 melanoma in mice. *J. Leukoc. Biol.* 90: 777–785.
45. Kakuta, S., Y. Tagawa, S. Shibata, M. Nanno, and Y. Iwakura. 2002. Inhibition of B16 melanoma experimental metastasis by interferon-gamma through direct inhibition of cell proliferation and activation of antitumour host mechanisms. *Immunology* 105: 92–100.

The Journal of Immunology

Endosomal Localization of TLR8 Confers Distinctive Proteolytic Processing on Human Myeloid Cells

Noriko Ishii, Kenji Funami, Megumi Tatematsu, Tsukasa Seya and Misako Matsumoto

J Immunol 2014; 193:5118-5128; Prepublished online 8 October 2014;
doi: 10.4049/jimmunol.1401375
http://www.jimmunol.org/content/193/10/5118

The Journal of Immunology is published twice each month by The American Association of Immunologists, Inc., 9650 Rockville Pike, Bethesda, MD 20814-3994.

Print ISSN: 0022-1767 Online ISSN: 1550-6606.